

case studies have been reported on the health outcomes of CNT-exposed workers. Although the toxicity of CNT has been studied both *in vivo* and *in vitro*, there is a paucity of toxicity and carcinogenicity data available for the health risk assessment of workers exposed to CNT. Recently, induction of mesotheliomas by intraperitoneal and intrascrotal injections of straight type MWCNT in p53 gene-deficient mice<sup>4)</sup> and male F344 rats<sup>5)</sup>, respectively, and asbestos-like pathogenicity by intraperitoneal injection of MWCNT in female mice<sup>6)</sup> have been reported. Mutation of the *k-ras* gene locus in the lungs of mice exposed by inhalation to SWCNT<sup>7)</sup> and positive clastogenicity and aneugenicity of MWCNT<sup>8)</sup> in Type II pneumocytes of female rats intratracheally instilled with MWCNT are also noteworthy. *In vitro* cytotoxicity studies using SWCNT and MWCNT have revealed varying degrees of cytotoxicity depending on physical dimensions such as length and width, agglomerated or dispersed state, functionalization and metal impurities<sup>9-20)</sup>. *In vitro* genotoxicity studies have demonstrated that SWCNT and MWCNT showed genotoxicity in a micronucleus assay<sup>8)</sup> and in a mutation assay with mouse embryonic stem cells<sup>20)</sup>, although bacterial mutagenicity was not shown for these nanomaterials<sup>22-24)</sup>.

Recent *in vivo*<sup>4-6)</sup> and *in vitro*<sup>11-13)</sup> toxicity studies have suggested that the hazardous effects of MWCNT fibers resemble those of asbestos fibers, because of the similarity in physical dimensions and biopersistence of MWCNT and asbestos<sup>25)</sup>. The present study was designed to examine the cytotoxicity and genotoxicity of MWCNT, including chromosome aberration, micronucleus induction, and mutagenicity at the hypoxanthine-guanine phosphoribosyltransferase (*hgprrt*) locus, as well as scanning electron microscopic (SEM) and light-microscopic observations of MWCNT-exposed cells, in an *in vitro* study using a Chinese hamster lung (CHL/IU) cell line and therefore to compare the cytotoxicity and genotoxicity of MWCNT with those of UICC chrysotile A (chrysotile) asbestos.

## Materials and Methods

### Chemicals

MWCNT was donated by MITSUI & Co. Ltd. (MWNT-7, Lot No. 061220, Tokyo, Japan). It was found in our previous study<sup>26)</sup> that the mean and SD of the fiber lengths were  $5.0 \pm 4.5 \mu\text{m}$  for MWCNT. Fibers longer than  $5 \mu\text{m}$  were found to occupy 38.9% of the total fibers counted, and the mean and SD of the fiber widths were  $88 \pm 5 \text{ nm}$ , resulting in an average ratio of 57. Chrysotile A of UICC (Union Internationale Contre le Cancer) was donated by Dr. M. Kudo, Occupational Health Research and Development Center, Japan Industrial Safety and Health Association. The length distribution of UICC chrysotile A was reported to be 20.7, 34.9, 23.1 and 15.2%

for 0.2–0.5, 0.5–1.0, 1–2 and 2–5  $\mu\text{m}$ , respectively<sup>27)</sup>, indicating that the distribution of fiber lengths in chrysotile was skewed apparently to shorter lengths than that in MWCNT. MWCNT and chrysotile were used without being purified or further sieved. It was also found in the previous study<sup>26)</sup> that MWCNT contained 4,400 ppm (wt/wt) iron, 48 ppm chromium and 17 ppm nickel by graphite furnace atomic absorption spectrometric analysis. Eagle's MEM was purchased from GIBCO (Invitrogen Cell Culture, CA, USA), calf serum (CS) from JRH Biosciences (Kansas City, USA). Carboxymethyl cellulose sodium salt (CMC), dimethylsulfoxide (DMSO) and polyoxyethylene (20) sorbitan monooleate (Tween 80) were purchased from Wako Pure Chemical Industries, Ltd. (Osaka, Japan). Phosphate-buffered saline (PBS) was purchased from Nissui Pharmaceutical Co. Ltd. (Tokyo, Japan). Mitomycin C (MMC) and ethyl methanesulfonate (EMS) used as positive controls were purchased from Wako Pure Chemical Industries, Ltd. (Osaka, Japan). Ultra-pure water was manufactured in-house with a water purification system (Milli-Q synthesis A10, Millipore Corporation, MA, USA).

### Suspension and dispersion of MWCNT or chrysotile in solvent

Since MWCNT is water-insoluble and is agglomerated firmly to micron-sized particles, it must be suspended in an appropriate solvent and dispersed into isolated fibers by ultrasonication. The most suitable solvent was selected from the following 4 solvents, in combination with the 3-minute ultrasonication. 1) Direct suspension of MWCNT in Eagle's MEM supplemented with 10% heat-inactivated CS used as culture medium. 2) Suspension of MWCNT in a mixture of DMSO and the culture medium with a final concentration of DMSO in the culture medium suspending MWCNT of 0.5% (5.5 mg/ml; 70 mM). 3) Suspension of MWCNT in an aqueous solution containing Tween 80 followed by addition of the ultrasonicated suspension into the culture medium. The final concentration of Tween 80 in the culture medium suspending MWCNT was 0.1 mg/ml. 4) Suspension of MWCNT in CMC solution followed by addition of the ultrasonicated suspension into the culture medium. The final concentration of CMC in the culture medium suspending MWCNT was 1 mg/ml. All these solvents displayed no cytotoxicity in the range of the concentrations used here. Since in our preliminary experiment chrysotile was found to be wettable in water, chrysotile was suspended in ultra-pure water (milli-Q). This was added to the culture medium at final concentrations of 0.25 to 50  $\mu\text{g/ml}$  and ultrasonicated for 3 min. An ultrasonic homogenizer (VP-30S, 20 kHz, 300 W, TAITEC Co. Ltd., Tokyo, Japan) was used to ultrasonicate the suspensions of MWCNT or chrysotile. The time period of 3 min for the ultrasonication was

determined from the empirical relationship between the time periods of ultrasonication and dispersion of MWCNT as indicated by the size distribution of MWCNT in the DMSO/culture medium. A dynamic light scattering size (DLS) apparatus, Zetasizer Nano DLS Analyzer (Malvern, Worcestershire, UK), was used to measure the size distribution of MWCNT in the suspension. The vertical axis of intensity against hydrodynamic diameters, shown in Fig. 1A and 1B, represents the normalized intensity of the light scattered through the aqueous media containing MWCNT, and was expressed as a percentage of total intensity (total area as 100%). The normalized intensity of scattered light depends on both the number of particles and their sizes.

### Cells

A clonal sub-line derived from the lung of a newborn female Chinese hamster (CHL/IU) was donated by the National Institute of Health Sciences (Tokyo, Japan). The cells were cultured in Eagle's MEM supplemented with 10% heat-inactivated CS (culture medium), and grown in a monolayer. The modal chromosome number was 25 and the doubling time was approximately 15 h<sup>28)</sup>.

### Colony formation assay for cytotoxicity

One hundred cells (20 cells/ml  $\times$  5 ml) of single cell suspension were seeded in a 60-mm plastic culture dish, incubated in a culture medium for 24 h, and then replaced with the test substance suspended in culture medium. The cells were exposed to MWCNT at 12.5 to 400  $\mu$ g/ml or chrysotile at 0.25 to 50  $\mu$ g/ml for 7 days. Then, the cells were fixed with ethanol for 5 min and stained with 0.1% crystalviolet for 20 min, and colonies were counted under a microscope. The percentage of surviving cells (viability) was calculated by dividing the number of colonies formed during MWCNT treatment by the number of colonies in the control medium and multiplying by 100.

### Lactate dehydrogenase (LDH) assay for cytotoxicity

One hundred thousand cells (20,000 cells/ml  $\times$  5 ml) were seeded in a 60-mm plastic culture dish, incubated in a culture medium for 48 h, and then replaced with the test substance suspended in culture medium. The cells were exposed to MWCNT at 12.5 to 400  $\mu$ g/ml or chrysotile at 10  $\mu$ g/ml for 24 h. The medium containing the test substance was then centrifuged at 13,000 rpm (16,000  $\times$  g) for 5 min. The LDH concentration in the supernatant was measured by a Clinical Analyzer (7070, Hitachi, Ltd. Tokyo, Japan). The remaining cells in the dish were transferred to a 0.1% tritonX-100 solution to extract LDH inside the cells, and then centrifuged at 13,000 rpm for 5 min. The LDH concentration in the supernatant was measured by the same method as described above. The LDH release rate was calculated by dividing the concentration of LDH in the test substance

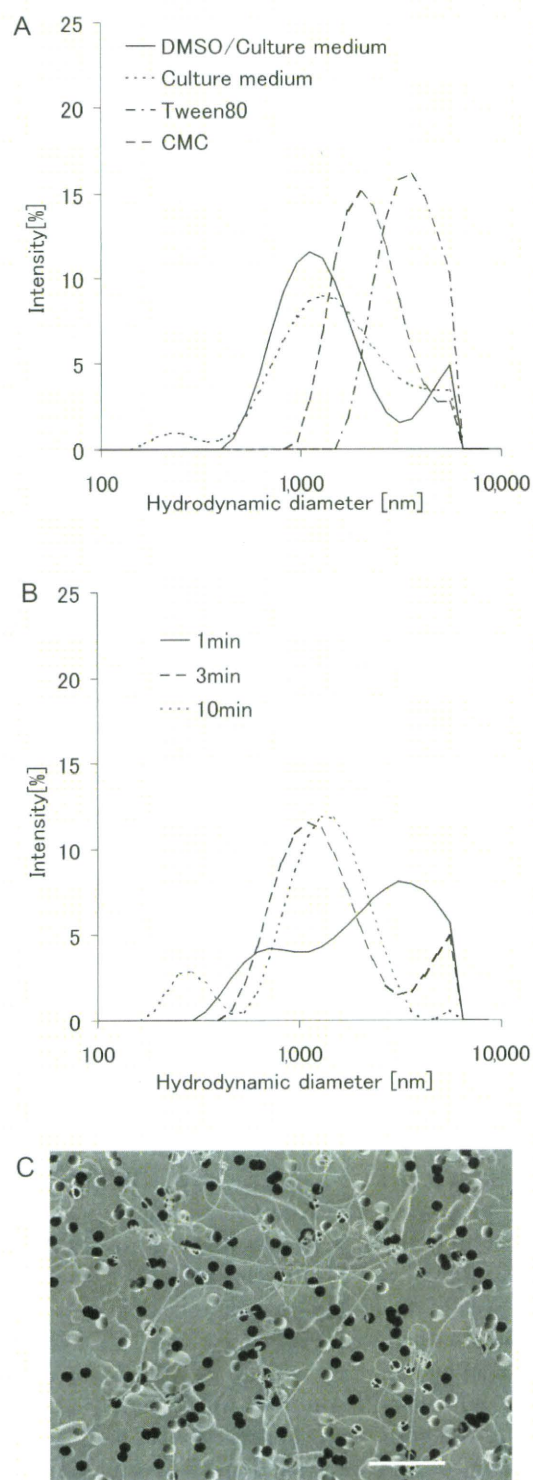


**Fig. 1.** Size distribution curves of MWCNT suspended in various solvents (A) and in DMSO/culture medium ultrasonicated for different durations with an ultrasonic homogenizer (B). A SEM image (C) showing good dispersion of agglomerated MWCNT into single, isolated fibers in the DMSO/culture medium after 3 min ultrasonication. Bar indicates 5  $\mu$ m.

suspended in culture medium by the total concentration of LDH inside (in the triton X-100 solution) and outside the cells and multiplying by 100.

#### *Chromosome aberration assay*

One hundred thousand cells (20,000 cells/ml  $\times$  5 ml) were seeded in a 60-mm plastic culture dish, incubated in a culture medium for 24 h, and then replaced with test substance suspended in culture medium. The cells were exposed to MWCNT at 0.078 to 80  $\mu\text{g/ml}$  or chrysotile at 0.8 to 20  $\mu\text{g/ml}$  for 24 or 48 h. DMSO at 0.5% or ultra-pure water at 5% served as a negative control and MMC at 0.04  $\mu\text{g/ml}$  as a positive control. Treatment concentrations of MWCNT or chrysotile were determined on the basis of the preliminary chromosome aberration assay. For chromosome preparation, colcemid at a final concentration of 0.2  $\mu\text{g/ml}$  was added to the culture medium 2 h before cell harvesting. Chromosomes were prepared by the air-drying method and stained with 2% Giemsa. The cytotoxicity was assessed by counting the trypan blue-stained cells as the dead ones, and expressed as a growth index by dividing the number of viable cells after 24- or 48-hour treatment with MWCNT or chrysotile by that of the respective negative control. The frequency of the cells with various types of structural aberrations including chromatid break, chromatid exchange, chromosome break, chromosome exchange and others (fragmentations except pulverization), for each dose in a 200 well-spread metaphase (100 metaphase/culture), as well as the cells with numerical aberration (polyploidy) were scored.

#### *Micronucleus assay*

Twenty-four thousand cells (12,000 cells/ml  $\times$  2 ml) were seeded in a 35-mm plastic culture dish, incubated in a culture medium for 24 h, and then replaced with the test substance suspended in culture medium. The cells were exposed to MWCNT at 0.02 to 5.0  $\mu\text{g/ml}$  or chrysotile at 0.1 to 1.6  $\mu\text{g/ml}$  for 48 h. DMSO at 0.5% or ultra-pure water at 5% served as a negative control and MMC at 0.01  $\mu\text{g/ml}$  as a positive control. Treatment concentrations of MWCNT or chrysotile were determined on the basis of the preliminary micronucleus assay. The cells were washed with PBS, fixed with 10% formaline and stained by mounting with 40  $\mu\text{g/ml}$  acridine orange and 10  $\mu\text{g/ml}$  DAPI solution. Immediately after the staining, the cells were observed with fluorescence microscopy using blue excitation, and evaluated for the number of cells having micronuclei, bi-nuclei and multi-nuclei having more than two nuclei in 2,000 intact interphase cells (1,000 cells/culture). The cytotoxicity was expressed as a growth index by dividing the number of viable cells after the 48-hour treatment with MWCNT or chrysotile by that of the respective negative control. Micronucleus was defined as having less than one-fourth of the diameter of the main nucleus. Numbers of bi-nucleated cells and mitotic cells as well as multi-nucleated

cells having more than two nuclei appearing in the same microscopic field were also counted.

#### *Mutation assay at the hprt locus*

Three-hundred thousand cells (30,000 cells/ml  $\times$  10 ml) were seeded in a 100-mm plastic culture dish, incubated in a culture medium for 24 h, and then replaced with the test substance suspended in culture medium. The cells were exposed to MWCNT at 6.3 to 100  $\mu\text{g/ml}$  or chrysotile at 1.56 to 25  $\mu\text{g/ml}$  for 48 h. DMSO at 0.5% or ultra-pure water at 5% served as a negative control and EMS at 200  $\mu\text{g/ml}$  as a positive control. Treatment concentrations of MWCNT or chrysotile were determined on the basis of the preliminary mutation assay. Then, the cells were rinsed with PBS and incubated in normal medium for a mutation expression time of 6 days. After the 6-day incubation, the cells were treated with trypsin, and 40,000 cells were transferred to each of twenty 60-mm culture dishes in medium containing 6-thioguanine (6-TG) for mutation selection. One hundred cells transferred to each of three 60-mm culture dishes in normal medium were used for cell viability assessment. After incubating for 10 days, the cell colonies formed were fixed with ethanol and stained with 5% Giemsa, and the number of 6-TG-resistant colonies was counted. The mutation frequency rate was expressed as the scored number of 6-TG-resistant cells per  $10^6$  cells corrected by the cell viability.

#### *Light-microscopic and SEM observations of cells exposed to MWCNT or chrysotile and MWCNT in the suspension*

The cells were exposed to MWCNT or chrysotile for 48 h. For light-microscopic observation, the cells exposed to MWCNT were fixed with methanol, and stained with 5% Giemsa. The chrysotile-exposed cells were fixed with methanol and observed under a phase-contrast microscope. For the SEM cell observation, the cells were pre-fixed in 1% glutaraldehyde in PBS, rinsed 4 times in PBS, and dehydrated using increasing concentrations of ethanol. After ethanol was replaced with *t*-butanol, the samples were subjected to critical point drying and sputter-coated with Pt. The cells and MWCNT or chrysotile were examined by SEM (SU-8000, Hitachi, Ltd., Tokyo, Japan). In order to examine whether MWCNT was dispersed in the culture medium, MWCNT was suspended in the DMSO/culture medium at 400  $\mu\text{g/ml}$  and ultrasonicated for 3 min. Then, the suspension was diluted to 1/10 in the medium, dripped onto an Isopore Track-Etched membrane filter (Millipore, Bedford, USA) and dried. After the filter was sputter-coated with Pt, MWCNT was observed by SEM.

#### *Statistical analysis*

The statistical significance of the dose-response relationship was tested by the Cochran-Armitage test.

Fisher's exact test was used for statistical comparisons between data of the dosed-groups and the respective controls. *p* values of less than 0.05 were considered to be statistically significant. A positive response showing mutagenicity at the *hprt* locus was judged as being biologically significant, when the mutation rate of the cells exposed to MWCNT or chrysotile was 2-fold greater than the negative control.

## Results

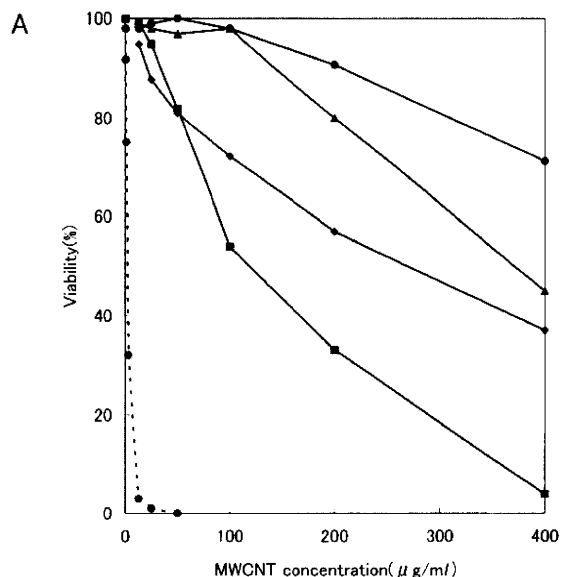
### Suspension and dispersion of MWCNT or chrysotile in solvent

In the present study, the distribution of hydrodynamic diameters of MWCNT in the suspension as assessed by the DLS measurement was used as an indicator of the MWCNT dispersion in the suspension. As shown in Fig. 1A, the principal peak was shifted toward smaller hydrodynamic diameters in the following order of the solvents: DMSO/culture medium > culture medium > CMC > Tween 80. This result indicates that MWCNT was dispersed more finely in DMSO/culture medium than in culture medium, CMC or Tween 80, when the ultrasonication duration was fixed at 3 minute. As shown in Fig. 1B, the 3- or 10-minute ultrasonication was found to decrease the hydrodynamic diameters of MWCNT more finely than the 1-minute ultrasonication. Besides, a small peak of 300 nm in the hydrodynamic diameter appeared after the 10-minute ultrasonication. A SEM image (Fig. 1C) revealed that MWNT was not agglomerated but dispersed into single, isolated fibers in the DMSO/culture medium after the 3-minute ultrasonication.

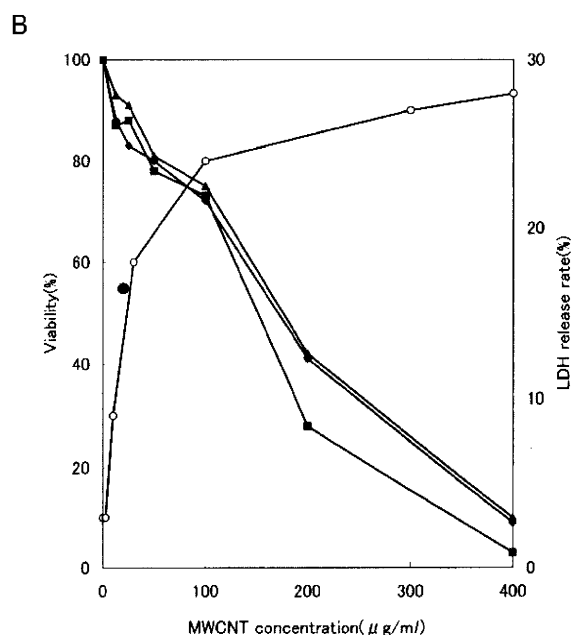
### Cytotoxicity

Figure 2A shows the effects of solvents used for the MWCNT suspension on cytotoxicity as evaluated by a colony formation assay with CHL/IU cells. The cell viability decreased with an increase in dose levels of MWCNT for all the solvents, and the cell viability tended to decrease in the following order: DMSO/culture medium > culture medium > Tween 80 > CMC. DMSO/culture medium exhibited the most potent cytotoxicity of MWCNT among the four solvents, suggesting that addition of DMSO to the culture medium (MEM+10% CS) helped to assure good dispersion of hydrophobic substances leading to potent toxicity. The dose-response curves of the cytotoxicities of chrysotile and MWCNT (Fig. 2A) revealed that the cytotoxicity of chrysotile was much more potent than that of MWCNT, when evaluated by the colony formation assay.

Figure 2B shows effect of ultrasonication duration on the cytotoxicity of MWCNT as evaluated by the colony formation assay. After 3-minute ultrasonication, MWCNT tended to exhibit more potent cytotoxicity at dose levels greater than 100  $\mu\text{g/ml}$  than after 1- or 10-minute



Effect of solvent used for MWCNT suspension on its cytotoxicity with CHL/IU cells. —●— culture medium, —■— DMSO/culture medium, —▲— Tween 80, —○— 1% CMC, —●— chrysotile (water).



Effect of ultrasonication of MWCNT on its cytotoxicity with CHL/IU cells. —●— 1 min (colony), —■— 3 min (colony), —▲— 10 min (colony), —○— 3 min (LDH), ● : LDH release rate of chrysotile at 10  $\mu\text{g/ml}$ .

**Fig. 2.** Dose-response curves of cytotoxicity induced by MWCNT suspended in various solvents and chrysotile in a colony formation assay (A), and of cytotoxicity induced by MWCNT ultrasonicated for different duration in a colony formation assay together with the dose-response curve of LDH release rate induced by MWCNT (B). The LDH release rate of chrysotile at 10  $\mu\text{g/ml}$  is indicated by a closed circle.

**Table 1.** Structural and numerical chromosome aberrations of MWCNT and chrysotile with CHL/IU cells

Treatment time (h)	Concentration ( $\mu\text{g}/\text{ml}$ )	Cell No.	Percent (%) of cells showing structural chromosome aberrations					total	Percent (%) of cells showing polyploids		Growth index (%)
			ctb	cte	csb	cse	other		Cell No.	polyploidy	
<b>MWCNT</b>											
24	0	200	0	0	0	0	0	0	201	0.5	100
	1.3	200	0	0	0	0	0	0	203	1.5	76
	5.0	200	0	0	0	0	0	0	207	3.4*	62
	20	200	0	0	0	0	0	0	234	14.5**	56
	80	200	0	0	0	0	0	0	242	17.4**	50
	MMC	200	7	23.5	0	0	0	0	28.5**	200	0
48	0	200	0.5	0	0	0	0	0.5	202	1.0	100
	0.078	200	0.5	0	0	0	0	0.5	203	1.5	83
	0.31	200	0.5	0	0	0	0	0.5	204	2.0	74
	1.3	200	0	0	0	0	0	0	217	7.8**	67
	5.0	200	0	0	0	0	0	0	261	23.4**	59
	MMC	200	6.5	58.5	0	0	0	0	63**	200	0
<b>Chrysotile</b>											
24	0	200	0	1.5	0.5	0	0	2.0	201	0.5	100
	0.8	200	0.5	0.5	0	0	0	1.0	209	4.3*	80
	4.0	200	0.5	1.5	0	0	0	2.0	258	22.5**	69
	20	200	0	0	0	0	0	0	304	34.2**	42
	MMC	200	11	30	0	0	0	0	38.5**	201	0.5
48	0	200	0.5	0	0	0	0	0.5	201	0.5	100
	0.8	200	0.5	0.5	0	0	0	1.0	208	3.8*	96
	4.0	200	1.0	1.0	0	0.5	0	2.5	224	10.7**	81
	20	200	1.0	0.5	0	0.5	0	2.0	330	39.4**	42
	MMC	200	13	35.5	0	0.5	0	0	41.5**	201	0.5

Fisher's exact test: \*  $p < 0.05$ , \*\*  $p < 0.01$ . a) Cochran-Armitage test. ctb: chromatid break; cte: chromatid exchange; csb: chromosome break; cse: chromosome exchange; others: fragmentation etc. (except pulverization); MMC: Mitomycin C at  $0.04 \mu\text{g}/\text{ml}$ .

ultrasonication. On the basis of this result, the time period for ultrasonication of the MWCNT suspension was fixed at 3 min throughout the present study. Figure 2B also shows that both colony formation and LDH assays exhibited clear but different dose-response curves for cytotoxicity. It was also found that the LDH release rate of chrysotile at  $10 \mu\text{g}/\text{ml}$  was greater than that expected from the dose-response curve of MWCNT, indicating that chrysotile damaged the CHL/IU cells more severely than MWCNT on an equal mass basis.

#### Chromosome aberration

As shown in Table 1, neither MWCNT nor chrysotile

induced any type of structural chromosome aberrations for the 24- or 48-hour continuous treatment at the designated dose levels. On the other hand, both MWCNT and chrysotile induced numerical chromosome aberrations of polyploidy in a significantly dose-dependent manner as indicated by the Cochran-Armitage test. A significantly increased number of cells showing polyploidy was observed for MWCNT at  $5 \mu\text{g}/\text{ml}$  and above in the 24-hour treatment and at 1.3 and  $5 \mu\text{g}/\text{ml}$  in the 48-hour treatment. Chrysotile significantly induced higher polyploidy at lower dose levels than MWCNT did on an equal mass basis. The minimum dose levels of MWCNT and chrysotile for the significant induction of

**Table 2.** Micronucleus assay of MWCNT and chrysotile with CHL/IU cells

Concentration ( $\mu\text{g/ml}$ )	MN (%)	Other relevance (%)			Growth Index (%)
		Bi-N	Multi-N	MP	
<b>MWCNT</b>					
0	8.5	4.5	2.5	14.5	100
0.02	10.5	3.0	2.5	12.5	94
0.078	9.5	6.0	2.5	11.5	88
0.31	12.0	19.0**	5.0	12.0	79
1.3	13.0	27.5**	10.5**	10.0	73
5.0	14.0	63.5**	21.5**	9.5	63
Cochran- Armitage test	$p<0.05$	$p<0.01$	$p<0.01$	–	–
MMC	48.5**	9.5	5.0	9.5	–
<b>Chrysotile</b>					
0	16.0	4.0	2.5	30.0	100
0.1	17.0	4.0	4.5	27.5	98
0.2	22.5	7.5	4.5	25.5	99
0.4	24.0*	40.0**	12.5**	20.5	89
0.8	24.5*	52.5**	14.0**	22.0	86
1.6	30.5**	68.0**	32.5**	23.0	84
Cochran- Armitage test	$p<0.01$	$p<0.01$	$p<0.01$	–	–
MMC	82.0**	5.5	8.5**	21.5	–

Fisher's exact test. \*  $p<0.05$ , \*\*  $p<0.01$ . MN: micronucleated cell; Bi-N: bi-nucleated cell; Multi-N: multi-nucleated cell having more than two nuclei; MP: mitotic cell; MMC: Mitomycin C at 0.01  $\mu\text{g/ml}$ . Observed number of cells was 2,000 cells per dose.

polyploidy corresponded to those at which the cell viability, as indicated by the growth index, exceeded 60% for MWCNT and 80% for chrysotile. MMC, which was used as a positive control, did not induce the numerical chromosome aberration but significantly increased the frequency of structural chromosome aberrations which consisted primarily of chromatid break and exchange.

#### Micronucleus induction

As shown in Table 2, no statistically significant increase in the number of micronucleated cells was found at any dose level of MWCNT as compared with the negative control, although MWCNT exhibited a statistically significant dose-dependent micronucleus induction as indicated by the Cochran-Armitage test. Chrysotile showed a statistically significant increase in the number of micronucleated cells at 0.4  $\mu\text{g/ml}$  and above, in addition to a significant dose-response relationship for the micronucleated cells. However, it should be pointed out that the number of micronucleated cells induced by MWCNT or chrysotile at the maximum dose level increased by less than 2-fold as compared with the respective negative controls. This result indicates that the statistical increase is marginal. On the other hand, MWCNT significantly increased the numbers of bi-nucleated and multi-nucleated cells at 0.31  $\mu\text{g/ml}$  and

above and at 1.3  $\mu\text{g/ml}$  and above, respectively, as compared with the negative controls, and also in a dose-dependent manner as indicated by the Cochran-Armitage test. Notably, the numbers of bi-nucleated and multi-nucleated cells induced by MWCNT at 5.0  $\mu\text{g/ml}$  were increased 14- and 8.6-fold, respectively, as compared with the respective control levels. Chrysotile also significantly increased the bi-nucleated and multi-nucleated cells at 0.4  $\mu\text{g/ml}$  and above in a dose-dependent manner. Statistically significant induction of bi-nucleated cells by chrysotile occurred at approximately the same dose level as that by MWCNT on an equal mass basis. The numbers of bi-nucleated and multi-nucleated cells induced by chrysotile at 1.6  $\mu\text{g/ml}$  were increased 17- and 13-fold, respectively, as compared with the respective control levels. The minimum dose levels of MWCNT and chrysotile for the significant induction of bi-nucleated and multi-nucleated cells corresponded to those at which the cell viability as indicated by the growth index exceeded 70% for MWCNT and 80% for chrysotile. MMC markedly induced micronuclei without the formation of bi-nucleated cells.

#### Mutation at the *hprt* locus

Table 3 shows mutation rates and viabilities of CHL/IU cells exposed to MWCNT or chrysotile at different

**Table 3.** Mutagenicity of MWCNT and chrysotile at the *hprt* locus with CHL/IU cells

Concentration ( $\mu\text{g/ml}$ )	Viability(%)	Mutation rate per $10^6$ cells
<b>MWCNT</b>		
0	100	4.68
6.3	86	3.56
12.5	63	6.83
25	48	4.77
50	33	6.14
100	21	3.82
EMS	33	462*
<b>Chrysotile</b>		
0	100	5.53
1.56	73	7.38
3.13	54	6.63
6.25	43	5.33
12.5	23	2.32
25	17	1.53
EMS	48	325*

EMS: ethyl methanesulfonate at 200  $\mu\text{g/ml}$ . \*: Positive response.

dose levels. Neither MWCNT nor chrysotile was negative for the mutagenicity at the *hprt* locus with CHL/IU cells, although the exposures to MWCNT and chrysotile decreased the cell viabilities to 21% and 17%, respectively, in a dose-dependent manner. Exposure of CHL/IU cells to EMS, a positive control, at 200  $\mu\text{g/ml}$  induced clearly positive mutagenicity at the *hprt* locus.

#### Cellular uptake of MWCNT and chrysotile

Light-microscopic observation, shown in Fig. 3A, revealed that dispersed and isolated MWCNT fibers were internalized in CHL/IU cells and were localized in the cytoplasm. Long MWCNT fiber bridging two cells and a multi-nucleated cell noteworthy. Cellular internalization of MWCNT was confirmed by SEM observation, as shown in Fig. 3B. The cellular uptake of MWCNT fibers was incomplete, and Fig. 3B shows a MWCNT fiber of longer than 5  $\mu\text{m}$  penetrating into a cell in the highly magnified inset. Both phase-contrast microscopic and SEM observations also showed cellular uptake and localization of long chrysotile (Fig. 3C), and incomplete internalization and cytoplasmic penetration of chrysotile fibers longer than 10  $\mu\text{m}$  (Fig. 3D) in the same manner as MWCNT.

## Discussion

### Cytotoxicity

In the present study, MWCNT-exposed CHL/IU cells exhibited a dose-dependent increase in cytotoxicity as evaluated by both the colony formation and LDH assays. The degree of MWCNT-induced cytotoxicity was found

to depend on the solvent used for suspension of hydrophobic MWCNT and the ultrasonication duration of the MWCNT suspension. Suspension of MWCNT in DMSO/culture medium and subsequent 3-minute ultrasonication induced the highest MWCNT-induced cytotoxicity, giving the most sensitive dose-response relationship of cytotoxicity as evaluated by the colony formation assay. It was also found by DLS measurement that the hydrodynamic diameter of MWCNT decreased in the following order of solvents: Tween 80 > CMC > culture medium > DMSO/culture medium under a fixed condition of 3-minute ultrasonication; and hydrodynamic diameters decreased in the following order of ultrasonication duration: 1 min > 3 min = 10 min in the of DMSO/culture medium. Therefore, it can be inferred from the present results that the degree of MWCNT-induced cytotoxicity tended to increase with a decrease in the hydrodynamic diameter of MWCNT in the culture medium, presumably due to the effective dispersion of agglomerated MWCNT to isolated MWCNT by ultrasonication and also the solvent, containing DMSO and serum. DMSO has been reported to facilitate good dispersion of hydrophobic MWCNT<sup>(11)</sup> at 0.5% which is below the DMSO concentration that inhibited cellular death due to scavenging reactive oxygen species (ROS) at concentrations ranging from 140 to 280 mM<sup>(29)</sup>. Consistently, our SEM observation confirmed good dispersion of agglomerated MWCNT into single, isolated fibers in the DMSO/culture medium after the 3-minute ultrasonication (Fig. 1C). However, it should be pointed out that although the 10-minute ultrasonication produced

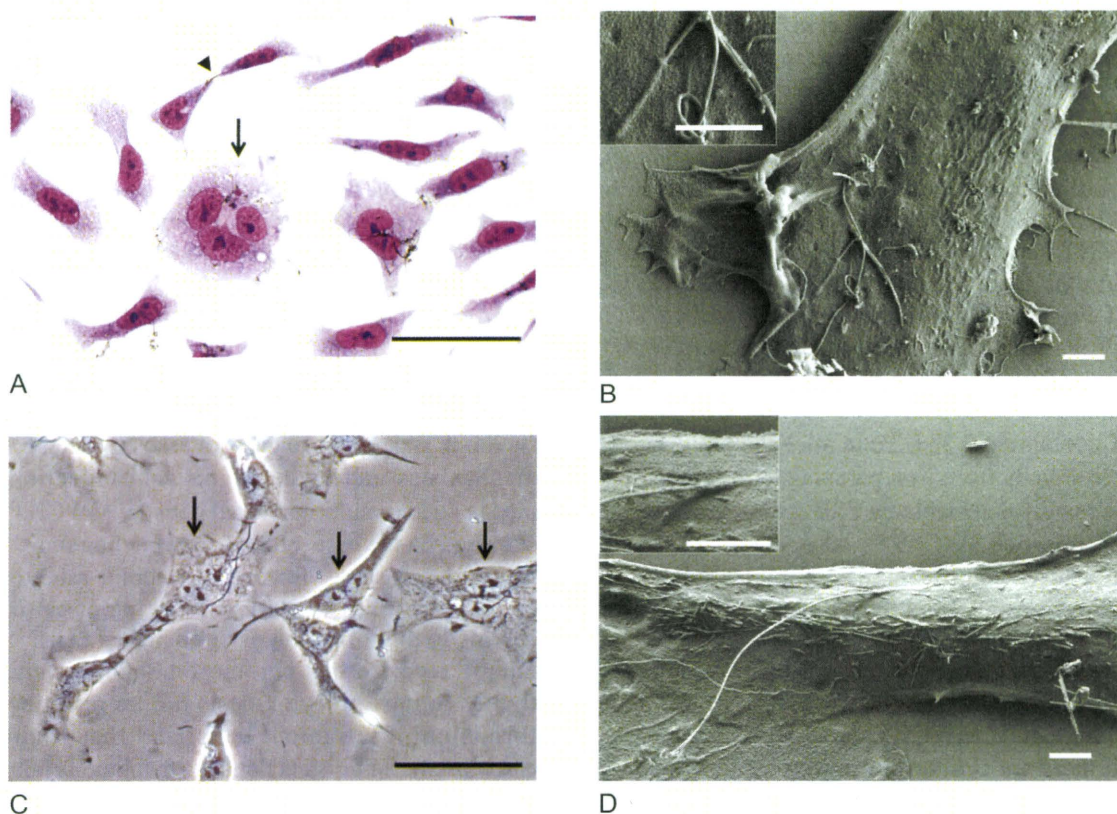


**Fig. 3.** CHL/IU cells exposed to MWCNT (A and B) or chrysotile (C and D). A: Light-microscopic image of the CHL/IU cells exposed to MWCNT at 4.0  $\mu\text{g/ml}$  for 48 h. A multi-nucleated cell is observed in the center (arrow), and a 20- $\mu\text{m}$  long MWCNT fiber on the upper side (arrowhead) bridges two cells. Bar indicates 50  $\mu\text{m}$ ; Giemsa stain. B: A SEM image showing single, isolated MWCNT fibers incompletely internalized into a cell. The inset is a higher magnification of the same cell to show the MWCNT fiber penetrating into the cell. Bars indicate 2  $\mu\text{m}$ . C: Phase-contrast microscopic image of cells exposed to chrysotile at 5.0  $\mu\text{g/ml}$  for 48 h. Several bi-nucleated CHL/IU cells are observed (arrows). Chrysotile fibers are localized in the cytoplasm. No staining; Bar indicates 50  $\mu\text{m}$ . D: A SEM image showing a single chrysotile fiber incompletely internalized into a CHL/IU cell. The inset is a higher magnification of the same cell showing the chrysotile fiber penetrating beneath the surface of the cell membrane. Bars indicate 2  $\mu\text{m}$ .

a submicron-sized, small peak of 300 nm in hydrodynamic diameter, the cytotoxicity of MWCNT after the 10-minute ultrasonication was less potent than that after the 3-minute ultrasonication. This result suggests that exposure of CHL/IU cells to the submicron-sized MWCNT at the relatively low levels does not enhance the cytotoxicity.

The present result that MWCNT induced dose-dependent release of LDH from CHL/IU cells is comparable with the finding of Muller *et al.*<sup>8)</sup> that MWCNT induced a dose-dependent increase in the release of LDH from rat lung epithelial (RLE) cells together with decreased mitochondrial activity in the same cells as measured with the dimethylthiazole-tetrazolium (MTT) assay. It has been generally recognized that cytotoxicity is causally related to cellular internalization of CNT<sup>30)</sup>, while cellular generation of ROS is involved in the mechanism of cytotoxicity for asbestos fibers<sup>31)</sup>, in

addition to internalization. However, it remains unclear whether the internalized CNT causes cytotoxicity through generation of ROS. Unpurified, iron-rich CNT but not purified CNT was reported to produce ROS in *in vitro* studies<sup>18-20)</sup>. Recently, Tabet *et al.*<sup>13)</sup> reported that MWCNT containing 2% iron decreased *in vitro* cell viability without internalization of MWCNT in human lung epithelial cells or production of intracellular oxidative responses as implied by RNA expression of different genes. It is noteworthy in the present study that both MWCNT and chrysotile were incompletely internalized in CHL/IU cells, resulting in cytoplasmic penetration of these two fibers, and localization in the cytoplasm (Fig. 3). Consistent with the present observation, cellular uptake of MWCNT has been demonstrated by light- and electron-microscopy<sup>9,10,14,18,21)</sup>. In this context, it is also interesting to note that *in vivo* exposure to long and thin MWCNT fibers caused frustrated phagocytosis and multi-nucleated



giant cells as reported by Poland *et al.*<sup>6)</sup> and incomplete cytoplasmic penetration of fibers as reported by Hubbs *et al.*<sup>32)</sup>. Therefore, MWCNT-induced cytotoxicity might be causally related to possible isolation and dispersion of agglomerated MWCNT in the DMSO/culture medium, which would facilitate uptake of MWCNT fibers into CHL/IU cells, possibly causing cellular impairment by the MWCNT fibers, and leading to growth inhibition and cellular death. Our previous study<sup>26)</sup> suggested, on the basis of Fe analysis and two *in vitro* and *in vivo* findings<sup>18, 19)</sup>, that an iron content of 0.44% in MWCNT exerts little effect on cell viability through Fe-induced ROS production, since pharyngeal aspiration of purified SWCNT containing 0.23% Fe in mice did not generate detectable signals from iron paramagnetic centers that would be readily detectable by ESR spectroscopy in the unrefined, iron-rich SWCNT<sup>18)</sup>. Also, iron-rich SWCNT (26% Fe) caused significant loss of intracellular GSH and accumulation of lipid hydroxides in RAW 264.7 macrophages as compared with iron-stripped SWCNT (0.23% Fe)<sup>19)</sup>. In this context, it was noteworthy in the present study that the cytotoxicity of chrysotile was more potent than that of MWCNT on an equal mass basis, although there are similarities in iron content and size distribution between MWCNT and chrysotile fibers<sup>25-27)</sup>. The surface properties of MWCNT as well as its physical dimension may play important roles in its cytotoxicity, as suggested by Tian *et al.*<sup>16)</sup>.

#### Genotoxicity

The *in vitro* genotoxicity of MWCNT found in the present study can be characterized by numerical but not structural chromosome aberration. Chromosomes showed polyploidy, and significantly increased numbers of bi-nucleated and multi-nucleated cells without clear micronucleus induction, as well as negative *hgp*rt mutagenicity. Chrysotile exhibited genotoxicity which was essentially the same as MWCNT, except for marginal but significant induction of micronuclei.

It has been reported that MWCNT shows negative bacterial mutagenicity in the presence and absence of metabolic activation<sup>22-24)</sup>. The present *hgp*rt mutagenicity assay can detect gene mutation in mammalian cells and confirmed the negative mutagenicity of MWCNT and chrysotile for CHL/IU cells as demonstrated by the bacterial mutagenicity assay. It is indicated, therefore, that neither MWCNT nor chrysotile interact directly with DNA.

The present results for MWCNT in the chromosome aberration assay can be contrasted with the findings of Muller *et al.*<sup>8)</sup> that MWCNT statistically increased the numbers of bi-nucleated MCF-7 cells containing centromere-positive and -negative micronuclei, and that the frequency of micronucleated cells of both RLE and human breast carcinoma (MCF-7) exposed to MWCNT

was increased in a dose-dependent manner. Their former finding with the fluorescence *in situ* hybridization (FISH) using a human pancentromeric probe is considered to be suggestive of the occurrence of both clastogenic and aneugenic events induced by MWCNT. However, the present results from the chromosome aberration and micronucleus induction assays revealed that MWCNT induces polyploidy but not micronuclei in a manner similar to chrysotile, while both MWCNT and chrysotile significantly increased the numbers of bi-nucleated and multi-nucleated cells. Since the distribution of lengths of MWCNT fibers was skewed to longer lengths than that for chrysotile, and since the long fibers of MWCNT were similar in appearance to those of asbestos fibers<sup>6, 25-27)</sup>, the mechanisms underlying significant induction of bi-nucleated and multi-nucleated cells by MWCNT can be surmised on the basis of the following literature. Jensen *et al.*<sup>33)</sup> demonstrated that long crocidolite asbestos fibers cause polyploidy by sterical blocking of cytokinesis, leading to the formation of bi-nucleated cells. Shi and King<sup>34)</sup> reported that chromosome non-disjunction is tightly coupled to cytokinesis failure resulting in the formation of tetraploid cells, and that coupling of chromosome non-disjunction with cytokinesis failure may potentiate mis-segregation during subsequent cell division, leading ultimately to the formation of aneuploid cells through multipolar mitosis of tetraploid cells. Taking these findings together, the significant induction of polyploidy without clear micronucleus induction by MWCNT, through the formation of bi-nucleated and multi-nucleated cells, is considered to result from the interference of long and thin MWCNT and chrysotile fibers with components of the mitotic spindle during chromosome segregation or from sterical blocking of cytokinesis. Our inference is consistent with the microscopic observation of Mangum *et al.*<sup>35)</sup> that a small fraction of alveolar macrophages from the lung of SWCNT-exposed rats was bridged by intracellular SWCNT that extended into the cytoplasm of two macrophages. It can be suggested, therefore, that the genotoxicity of long and thin MWCNT might be causally related to indirect interactions of MWCNT with DNA causing genomic instability such as aneugenic events, rather than direct interactions of MWCNT with DNA causing mutation and clastogenic events, neither of which were observed in the present study. Long MWCNT fibers have been reported to cause mesotheliomas in mice<sup>4)</sup> and rats<sup>5)</sup> and to behave like long asbestos fibers in the mouse peritoneal cavity<sup>6)</sup>. However, Muller *et al.*<sup>36)</sup> reported no significant induction of mesotheliomas in a 2-year bioassay in the peritoneal cavity of rats that received a single intraperitoneal injection of MWCNT, whereas crocidolite induced mesothelioma. Since the MWCNT that Muller *et al.* used was reported to contain short and tangled fibers of about 0.7  $\mu\text{m}$  in length<sup>36)</sup>, it can be

suggested that long (>5  $\mu\text{m}$ ) and straight MWCNT fibers elicit the carcinogenic response. Further study is urgently needed to explore possible causative factors such as physical and physicochemical properties of MWCNT, using in vitro assay systems, such as a cell transformation assay that might reflect the initiation and promotion stages of early carcinogenesis by MWCNT better than the genotoxicity assays used in the present study.

## Conclusions

Cytotoxicity of MWCNT depended on the solvent used for suspension of MWCNT and the ultrasonication duration of the suspension, suggesting that the cytotoxicity is causally related to dispersion and isolation of agglomerated MWCNT. The cytotoxicity of chrysotile was greater than that of MWCNT. The genotoxicity of MWCNT and chrysotile was characterized by negative *hgp*rt mutagenicity, insignificant induction of micronuclei, the formation of polyploidy without structural chromosome aberration, and increased numbers of bi-nucleated and multi-nucleated cells. SEM observation showed that MWCNT and chrysotile were incompletely internalized in the cells and localized in the cytoplasm. It was suggested that the genotoxicity of MWCNT and chrysotile may arise not from direct interaction with DNA, but from the physical interference of these two fibers with biological processes during cytokinesis.

*Acknowledgment:* The present study was supported in part by a Grant-in-Aid for Scientific Research from the Ministry of Health, Labour and Welfare of Japan.

## References

- Martin CR, Kohli P. The emerging field of nanotube biotechnology. *Nat Rev Drug Discov* 2003; 2: 29–37.
- Toray Corporate Business Research, INC. Report on the survey of production and use of nanomaterials in Japan, -Fy 2008- (in Japanese).
- Han JH, Lee EJ, Lee JH, et al. Monitoring multiwalled carbon nanotube exposure in carbon nanotube research facility. *Inhal Toxicol* 2008; 20: 741–9.
- Takagi A, Hirose A, Nishimura T, et al. Induction of mesothelioma in p53+/- mouse by intraperitoneal application of multi-wall carbon nanotube. *J Toxicol Sci* 2008; 33: 105–16.
- Sakamoto Y, Nakae D, Fukumori N, et al. Induction of mesothelioma by a single intrascrotal administration of multi-wall carbon nanotube in intact male Fischer 344 rats. *J Toxicol Sci* 2009; 34: 65–76.
- Poland CA, Duffin R, Kinloch I, et al. Carbon nanotubes introduced into the abdominal cavity of mice show asbestos-like pathogenicity in a pilot study. *Nature Nanotechnol* 2008; 3: 423–8.
- Shvedova AA, Kisin E, Murray AR, et al. Inhalation vs. aspiration of single-walled carbon nanotubes in C57BL/6 mice: inflammation, fibrosis, oxidative stress, and mutagenesis. *Am J Physiol Lung Cell Mol Physiol* 2008; 295: 552–65.
- Muller J, Decordier I, Hoet PH, et al. Clastogenic and aneugenic effects of multi-wall carbon nanotubes in epithelial cells. *Carcinogenesis* 2008; 29: 427–34.
- Monteiro-Riviere NA, Nemanich RJ, Inman AO, Wang YY, Riviere JE. Multi-walled carbon nanotube interaction with human epidermal keratinocytes. *Toxicol Lett* 2005; 155: 377–84.
- Sato Y, Yokoyama A, Shibata K, et al. Influence of length on cytotoxicity of multi-walled carbon nanotubes against human acute monocytic leukemia cell line THP-1 in vitro and subcutaneous tissue of rats in vivo. *Mol Biosyst* 2005; 1: 176–82.
- Soto K, Garza KM, Murr LE. Cytotoxic effects of aggregated nanomaterials. *Acta Biomater* 2007; 3: 351–8.
- Hirano S, Kanno S, Furuyama A. Multi-walled carbon nanotubes injure the plasma membrane of macrophages. *Toxicol Appl Pharmacol* 2008; 232: 244–51.
- Tabet L, Bussy C, Amara N, et al. Adverse effects of industrial multiwalled carbon nanotubes on human pulmonary cells. *J Toxicol Environ Health, Part A* 2009; 72: 60–73.
- Simon-Deckers A, Gouget B, Mayne-L'hermite M, Herlin-Boime N, Reynaud C, Carriere RM. In vitro investigation of oxide nanoparticle and carbon nanotube toxicity and intracellular accumulation in A549 human pneumocytes. *Toxicology* 2008; 253: 137–46.
- Manna SK, Sarkar S, Barr J, et al. Single-walled carbon nanotube induces oxidative stress and activates nuclear transcription factor -kappaB in human keratinocytes. *Nano Lett* 2005; 5: 1676–84.
- Tian F, Cui D, Schwarz H, Estrada GG, Kobayashi H. Cytotoxicity of single-wall carbon nanotubes on human fibroblasts. *Toxicol In Vitro* 2006; 20: 1202–12.
- Jacobsen NR, Pajana G, White P, et al. Genotoxicity, cytotoxicity, and reactive oxygen species induced by single-walled carbon nanotubes and C (60) fullerenes in the FEI-Mutatrade markMouse lung epithelial cells. *Environ Mol Mutagen* 2008; 49: 476–87.
- Pulskamp K, Diabate S, Krug HF. Carbon nanotubes show no sign of acute toxicity but induce intracellular reactive oxygen species in dependence on contaminants. *Toxicol Lett* 2007; 168: 58–74.
- Shvedova AA, Castranova V, Kisin ER, et al. Exposure to carbon nanotube material: assessment of nanotube cytotoxicity using human keratinocyte cells. *J Toxicol Environ Health, Part A* 2003; 66: 1909–26.
- Kagan VE, Tyurina YY, Tyurin VA, et al. Direct and indirect effects of single walled carbon nanotubes on RAW 264.7 macrophages: role of iron. *Toxicol Lett* 2006; 165: 88–100.
- Zhu L, Chang DW, Dai L, Hong Y. DNA damage induced by multiwalled carbon nanotubes in mouse embryonic stem cells. *Nano Lett* 2007; 7: 3592–7.
- Miyawaki J, Yudasaka M, Azami T, Kubo Y, Iijima S. Toxicity of single-walled carbon nanohorns. *ACS Nano*

- 2000; 2: 213–26.
- 23) Di Sotto A, Chiaretti M, Carru GA, Belluci S, Mazzanti G. Multi-walled carbon nanotubes: lack of mutagenic activity in the bacterial reverse mutation assay. *Toxicol Lett* 2009; 184: 192–7.
- 24) Wirtzner U, Herbold B, Voetz M, Ragot J. Studies on the in vitro genotoxicity of baytubes, agglomerates of engineered multi-walled carbon-nanotubes (MWCNT). *Toxicol Lett* 2009; 186: 160–5.
- 25) Murr LE, Soto KF. TEM comparison of chrysotile (asbestos) nanotube and carbon nanotubes. *J Mater Sci Lett* 2004; 39: 4941–7.
- 26) Takaya M, Serita F, Yamazaki K, et al. Characteristics of multiwall carbon nanotubes for an intratracheal instillation study with rats. *Ind Health* 48 (In press).
- 27) Langer AM, Nolan RP. Chrysotile: its occurrence and properties as variables controlling biological effects. *Ann Occup Hyg* 1994; 38: 427–51.
- 28) Ishidate M Jr., Odashima S. Chromosome tests with 134 compounds on Chinese hamster cells in vitro—a screening for chemical carcinogens. *Mutat Res* 1977; 48: 337–54.
- 29) Pourahmad J, O'Brien PJ. A comparison of hepatocyte cytotoxic mechanisms for Cu<sup>2+</sup> and Cd<sup>2+</sup>. *Toxicology* 2000; 143: 263–73.
- 30) Jaurand MC, Renier A, Daubriac J. Mesothelioma: do asbestos and carbon naotubes pose the same health risk? *Particle and Fibre Toxicol* 2009; 6: 1–16.
- 31) Manning CB, Vallyathan V, Mossman BT. Diseases caused by asbestos: mechanisms of injury and disease development. *Int Immunopharmacol* 2002; 2: 191–200.
- 32) Hubbs A, Mercer RR, Coad JE, et al. Persistent pulmonary inflammation, airway mucous metaplasia and migration of multiwalled carbon nanotubes from the lung after subchronic exposure. *The Toxicologist* 2009; 108: 457.
- 33) Jensen CG, Jensen LC, Rieder CL, Cole RW, Ault JG. Long crocidolite asbestos fibers cause polyploidy by sterically blocking cytokinesis. *Carcinogenesis* 1996; 17: 2013–21.
- 34) Shi Q, King RW. Chromosome nondisjunction yields tetraploid rather than aneuploid cells in human cell lines. *Nature* 2005; 437: 1038–42.
- 35) Mangum JB, Turpin EA, Antao-Menezes A, Cesta MF, Bermudez E, Bonnerr JC. Single-walled carbon nanotube (SWCNT)—induced interstitial fibrosis in the lungs of rats is associated with increased levels of PDGF mRNA and the formation of unique intercellular carbon structures that bridge alveolar macrophages in situ. *Particle Fibre Toxicol* 2006; 3: 315–28.
- 36) Muller J, Delos M, Panin N, Rabolli V, Huaux F, Lison D. Absence of carcinogenic response to multiwall carbon nanotubes in a 2-year bioassay in the peritoneal cavity of the rat. *Toxicol Sci* 2009; 110: 442–8.

Letter

## Air purifiers that diffuse reactive oxygen species potentially cause DNA damage in the lung

Kosuke Kawamoto<sup>1</sup>, Itaru Sato<sup>1</sup>, Midori Yoshida<sup>2</sup> and Shuji Tsuda<sup>1</sup>

<sup>1</sup>Department of Veterinary Medicine, Iwate University, 3-18-8 Ueda, Morioka, Iwate 020-8550, Japan

<sup>2</sup>Division of Pathology, National Institute of Health Sciences, 1-18-1 Kamiyoga, Setagaya, Tokyo 158-8501, Japan

(Received August 18, 2010; Accepted September 7, 2010)

**ABSTRACT** — Several appliance manufacturers have recently released new type air purifiers that can disinfect bacteria, fungi and viruses by diffusing reactive oxygen species (ROS) into the air. In this study, mice were exposed to the outlet air from each of 3 air purifiers from different manufacturers (A, B, C), and the lung was examined for DNA damage, lipid peroxidation and histopathology to confirm the safety of these air purifiers. Neither abnormal behavior during exposure nor gross abnormality at necropsy was observed. No histopathological changes were also observed in the lung. However, significant increase of DNA damage was detected by the comet assay in the lung immediately after the direct exposure for 48 hr to models A and B, and for 16 hr to model B. As for model B, DNA migration was also increased by 2 hr exposure in a 1 m<sup>3</sup> plastic chamber but not by 48 hr exposure in a room (12.6 m<sup>3</sup>). Model C did not cause DNA damage. Lipid peroxidation and 8-hydroxy deoxyguanosine (8-OH-dG) was not increased under the conditions DNA damage was detected by the comet assay. The present results revealed that some models of air purifiers that diffuse ROS potentially cause DNA damage in the lung although the mechanism was left unsolved.

**Key words:** DNA damage, Air purifier, Reactive oxygen species, Air ion, Lung

### INTRODUCTION

Air purifiers are commonly used in a house, office, hospital, and so on. Conventional air purifiers only remove particulates such as house dust, pollens, and cigarette smoke by a filter, whereas new type ones have a function to disinfect bacteria, fungi and viruses. For these purposes, some models are equipped with an antibacterial filter or photocatalytic device, and some models diffuse air-ions into the room.

There are several studies on the bactericidal or virucidal effects of air-ions (Mitchell and King, 1994; Fan *et al.*, 2002; Tyagi *et al.*, 2008), and the underlying mechanism is suggested to be degeneration of surface proteins of organisms (Digel *et al.*, 2005). According to the manufacturer's information, active substance of the air purifiers is superoxide or hydroxyl radical, which is a member of reactive oxygen species (ROS). ROS are potentially toxic to living matters. There are few published studies on the safety of these air purifiers although several manufacturers have officially announced on the website that various toxicity tests including genotoxicity test have been conducted by contract research organizations.

In this study, therefore, mice were exposed to the outlet air from these air purifiers and the lung was examined for DNA damage, lipid peroxidation and histopathology to confirm their safety.

### MATERIALS AND METHODS

#### Animals and apparatus

Seven weeks old ICR male mice were purchased from CLEA Japan (Tokyo, Japan), and randomly divided into groups of 5 mice each. They were fed commercial feed (MF, Oriental Yeast, Tokyo, Japan) and tap water throughout the acclimation (1 week) and experimental periods freely. The animal room was kept at 22-24°C with 12 hr light/dark cycle. Animal experiments were conducted according to the guidelines for animal experiments of Iwate University.

Three models of household air purifiers from different manufacturers, A, B and C were tested. According to the manufacturer's information, model A diffuses negative (O<sub>2</sub><sup>-</sup>) and positive (H<sup>+</sup>) cluster ions, model B diffuses nanoparticles of water including hydroxyl radical, and model C diffuses electrolytic water mist that includes hydroxyl rad-

Correspondence: Shuji Tsuda (E-mail: s.tsuda@iwate-u.ac.jp)

ical and hypochlorous acid. Chemicals used without special mention were purchased from Wako Pure Chemical Industries (Osaka, Japan).

### Exposure and sampling

For models A and B, exposure was conducted in an air duct connected to their outlet (Fig. 1). Air flow was 0.8 m<sup>3</sup>/min for A and 1.0 m<sup>3</sup>/min for B at low mode (wind velocity < 0.5 m/sec). For model C, exposure was conducted in an incubator (45 × 46 × 46 cm), because it was not equipped with a fan; and fresh air was introduced into the incubator (0.03 m<sup>3</sup>/min) by an air pump during exposure. All of the air purifiers were set to the low mode. The exposures were conducted for 16 hr or 48 hr in respective rooms.

Model B was also tested under two other exposure conditions. (I) The air purifier was put on a side of a small room (12.6 m<sup>3</sup>, 2.1 × 2.5 × 2.4 m), and mice were exposed at the opposite side of the room for 48 hr. (II) The air purifier and animal cage were put in an air-tight plastic chamber (1.0 m<sup>3</sup>, 0.9 × 1.2 × 0.9 m) to conduct the exposure for 2 hr. Oxygen concentration in the plastic chamber remained practically the same (20.9–20.7%) during exposure.

Immediately after exposure, mice were sacrificed by cervical dislocation to collect the lung for the assessment of its damage.

### Assessment of lung damage

DNA damage was assessed by the *in vivo* comet assay and 8-hydroxy deoxyguanosine (8-OH-dG). The comet assay was conducted according to Tsuda *et al.* (2000) and Hashimoto *et al.* (2007), where 50 nuclei/tissue were measured for DNA migration and the mean migration was regarded as the individual level of DNA damage. 8-OH-dG was determined by HPLC equipped with an electrochemical detector. Detailed procedures were described in

the next section. Lipid peroxidation was estimated by thiobarbituric acid reactive substances (TBARS) and 8-isoprostane. TBARS were determined according to the method of Kikugawa *et al.* (1992) with a little modification. We omitted the solvent extraction with butanol-pyridine, because transparent samples could be obtained by addition of propanol followed by centrifugation at 3,000 rpm. 8-Isoprostane was determined by an EIA kit (Cayman Chemical, Ann Arbor, MI, USA). Left lobes of the lung were fixed in 10% neutral buffered formalin, routinely processed, and stained with hematoxylin eosin for histopathological examination. Dunnett's test or Student's *t* test was employed for the statistical analysis, and *P* value less than 0.05 was considered statistically significant.

### 8-OH-dG assay

Tissue sample (100–200 mg) was gently homogenized at 0°C with 2 ml of lysing solution (1% Triton X-100, 320 mM saccharose, 5 mM MgCl<sub>2</sub>, 0.005% BHT, 10 mM Tris, pH 7.5) using a Potter homogenizer. A portion of 1 ml was centrifuged at 600 g for 10 min at 4°C, and the supernatant was carefully discarded. The precipitate was resuspended in 1 ml of the lysing solution and centrifuged under the same conditions. This step was repeated once more. The precipitate was suspended in 0.3 ml of reaction solution (1% SDS, 5 mM Na<sub>2</sub>EDTA, 0.005% BHT, 10 mM Tris, pH 8.0) and incubated with 10 µl of proteinase K (17 mg/ml) at 37°C for 60 min. During the incubation, the sample was shaken vigorously every 10 min to facilitate the enzyme reaction.

After the incubation, the sample was centrifuged at 10,000 g for 5 min at 4°C. The supernatant (0.15 ml) was mixed with 0.3 ml of NaI (7.6 M NaI, 20 mM Na<sub>2</sub>EDTA, 40 mM Tris, pH 8.0) and 0.6 ml of isopropanol, stirred until filamentous DNA was deposited, and centrifuged at 10,000 g for 5 min at 4°C. The precipitate was resuspended in 1 ml of 70% ethanol and centrifuged under the same

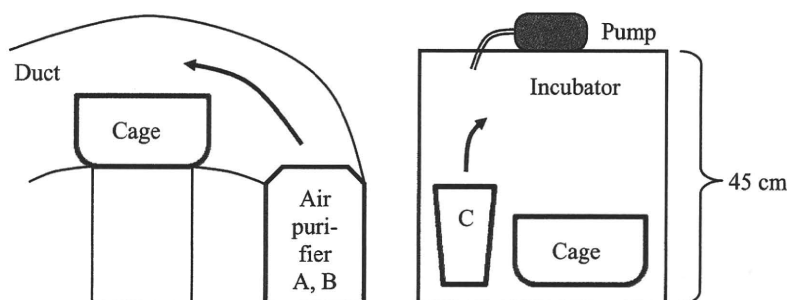


Fig. 1. Schematic diagram of the direct exposure.

## DNA damage in the lung caused by air purifier

conditions. This step was repeated once more. The supernatant was completely discarded to remove ethanol.

The precipitated DNA was dissolved in 0.1 ml of pure water, denatured in boiling water for 3 min, then cooled in ice water. Ten microliters of 200 mM acetic acid buffer (pH 5.3, 1 mM ZnCl<sub>2</sub>), nuclease P1 (100 U/ml, Yamasa Corporation, Chiba, Japan) and acid phosphatase (100 U/ml) were added to the DNA solution, incubated at 37°C for 30 min, then filtered with a centrifugal filter device (Ultrafree-MC, 0.45 µm, Millipore, Bedford, MA, USA) to obtain analytical sample for HPLC. Conditions of HPLC were as follows.

Apparatus : Shiseido Nanospace (Shiseido, Tokyo, Japan)  
 Column : Inertsil ODS, 3 µm, 3.0 × 50 mm (GL Science, Tokyo, Japan), 35°C  
 Eluent : 50 mM acetic acid buffer, pH 5.3, 5% methanol, 0.4 ml/min  
 Detector : UV (275 nm), ECD (Ox 0.6 V)

## Ozone measurement

Ozone concentration in the outlet air (model A and B) or in the incubator (model C) was measured by detection tubes (Komyo Rikagaku Kogyo, Kanagawa, Japan).

## RESULTS

Neither abnormal behavior during exposure nor gross abnormality at necropsy was observed. No changes were also detected by histopathological examination of the lung directly exposed to model A, B or C for 48 hr (pictures were omitted). The other exposure conditions were not allocated for histopathology.

DNA migration of the lung was significantly increased by 48 hr direct exposure to model A and B, and by 16 hr exposure to model B (Fig. 2). Sixteen hours exposure to model C was not examined, because this model did not increase DNA migration even after 48 hr exposure. As for model B, DNA migration was also increased by 2 hr exposure in a 1 m<sup>3</sup> plastic chamber but not by 48 hr expo-

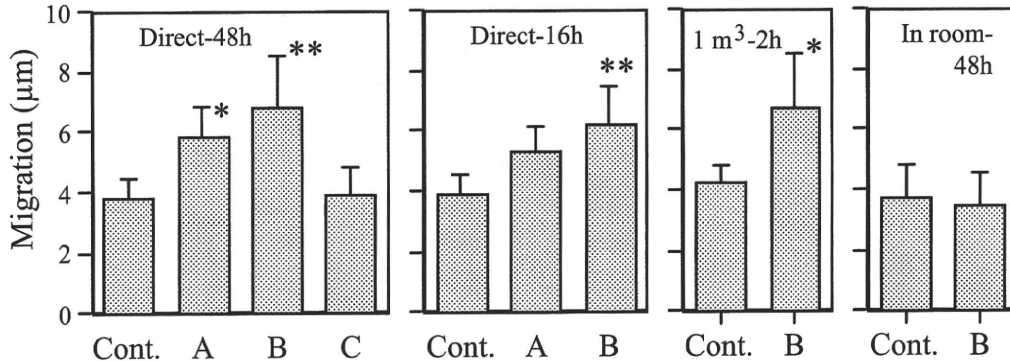


Fig. 2. DNA damage in the lung measured by the comet assay. Mean ± S.D. for 5 mice. \*:  $p < 0.05$ , \*\*:  $p < 0.01$ .

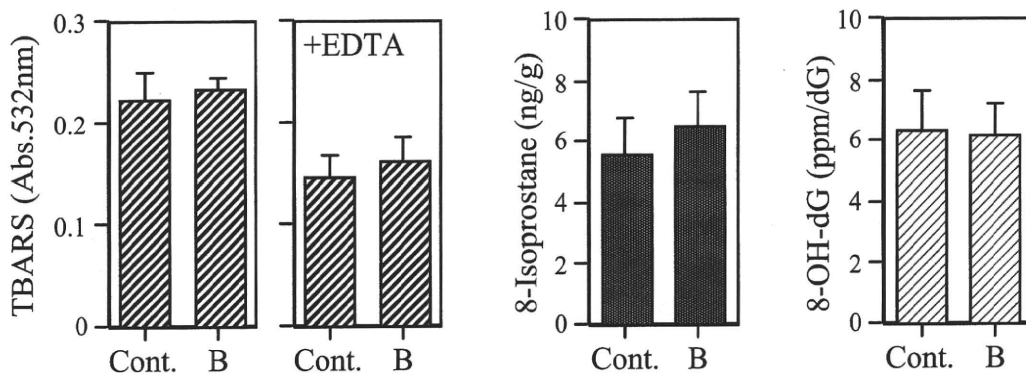


Fig. 3. Lipid peroxidation and 8-OH-dG in the lung of mice exposed directly to model B for 48 hr. Mean ± S.D. for 5 mice.

sure in a small room (Fig. 2).

TBARS, 8-isoprostane and 8-OH-dG were not affected by 48 hr direct exposure to model B (Fig. 3). The other exposure conditions were not examined for these endpoints because above condition caused most severe DNA damage.

Ozone concentration in the exposing air was lower than the detection limit (25 ppb) for all air purifiers tested.

## DISCUSSION

According to the instruction manuals, models A and B collaterally generate small amount of ozone. Ozone is a powerful oxidant that causes DNA damage as well as inflammatory reaction in the lung or pulmonary cultured cells (Victorin, 1992; Bornholdt *et al.*, 2002). An *in vivo* study using guinea pig has demonstrated that 72 hr exposure to 1 ppm ozone caused DNA single strand break (SSB) in tracheobronchial epithelial cells, but the same duration at 0.45 ppm did not cause SSB (Feng, 2002). Occupational exposure limit for ozone recommended by the Japan Society for Occupational Health is 0.1 ppm (JSOH, 2009). In this study, ozone levels in the exposing air were less than 0.025 ppm. Thus, ozone is not involved in the DNA damage caused by air purifiers. It was also demonstrated by histopathological examination that the DNA damage was not attributable to the cellular degeneration or necrosis.

Models A and B diffuse superoxide and hydroxyl radical, respectively, either of which can cause oxidative DNA damage such as modified base and strand break if it reaches the target site. However, they may not react directly with nuclear DNA of pulmonary cells because of their low membrane permeability and/or high reactivity. Thus, inhaled superoxide and hydroxyl radical might have primarily reacted with the epithelial cell lining fluid or cell membrane to cause lipid peroxidation, and indirectly attacked DNA through genotoxic products such as alkylperoxyl radicals, alkoxy radicals and reactive carbonyls (Burcham, 1998; Blair, 2008). Similar mechanism has been suggested for the development of ozone toxicity (Mehlman and Borek, 1987; Pryor and Church, 1991). However, there was no increase in the levels of TBARS and 8-isoprostane when mice were directly exposed to model B for 48 hr, while the DNA damage was observed. TBA method is a widely used conventional method to evaluate lipid peroxidation in living tissues and foods. 8-Isoprostane is a degradation product of arachidonic acid, and is reported to increase in high-oxygen environment (Vacchiano and Tempel, 1994). The negative results of both TBARS and 8-isoprostane suggest that lipid per-

oxidation may not be the main cause of the DNA damage. Another possibility may be hydrogen peroxide, a stable and penetrable ROS, which may have been generated before or after inhalation causing oxidative DNA damage of the lung. However, there was no change in the levels of 8-OH-dG, a marker of oxidative DNA damage, under the same conditions as mentioned above.

Model C, which diffuses electrolytic water mist by ultrasonic nebulizer, did not cause DNA damage. However, it is unclear whether the negative result was due to the unique mechanism of this model, because exposure conditions including ROS density were not equalized in this study.

Digel *et al.* (2005) examined bactericidal effects of plasma-generated air ions on several gram-positive strains. They found that the air ions did not damage bacterial DNA but denatured surface proteins. Bacterial cells are enveloped by thick cell wall which consists chiefly of peptidoglycan and teichoic acid. Therefore, the present results do not necessarily contradict their findings and revealed that some models of air purifiers that diffuse ROS potentially cause DNA damage in the lung under strong exposure conditions. However, the mechanism of DNA damage of the lung caused the air purifiers remains to be solved.

## REFERENCES

- Blair, I.A. (2008): DNA adducts with lipid peroxidation products. *J. Biol. Chem.*, **283**, 15545-15549.
- Bornholdt, J., Dybdahl, M., Vogel, U., Hansen, M., Loft, S. and Wallin, H. (2002): Inhalation of ozone induces DNA strand breaks and inflammation in mice. *Mutat. Res.*, **520**, 63-71.
- Burcham, P.C. (1998): Genotoxic lipid peroxidation products: their DNA damaging properties and role in formation of endogenous DNA adducts. *Mutagenesis*, **13**, 287-305.
- Digel, I., Temiz Artmann, A., Nishikawa, K., Cook, M., Kurulgan, E. and Artmann, G.M. (2005): Bactericidal effects of plasma-generated cluster ions. *Med. Biol. Eng. Comput.*, **43**, 800-807.
- Fan, L., Song, J., Hildebrand, P.D. and Forney, C.F. (2002): Interaction of ozone and negative air ions to control micro-organisms. *J. Appl. Microbiol.*, **93**, 144-148.
- Feng, S.F. (2002): Ozone-induced DNA single strand-breaks in guinea pig tracheobronchial epithelial cells *in vivo*. *Inhal. Toxicol.*, **14**, 621-633.
- Hashimoto, K., Takasaki, W., Sato, I. and Tsuda, S. (2007): DNA damage measured by comet assay and 8-OH-dG formation related to blood chemical analyses in aged rats. *J. Toxicol. Sci.*, **32**, 249-259.
- JSOH (Japan Society for Occupational Health) (2009): Recommendation of Occupational Exposure Limits. *J. Occup. Health*, **51**, 454-470.
- Kikugawa, K., Kojima, T., Yamaki, S. and Kosugi, H. (1992): Interpretation of the thiobarbituric acid reactivity of rat liver and brain homogenates in the presence of ferric ion and ethylenediaminetetraacetic acid. *Anal. Biochem.*, **202**, 249-255.

## DNA damage in the lung caused by air purifier

- Mehlman, M.A. and Borek, C. (1987): Toxicity and biochemical mechanisms of ozone. *Environ. Res.*, **42**, 36-53.
- Mitchell, B.W. and King, D.J. (1994): Effect of negative air ionization on airborne transmission of Newcastle disease virus. *Avian Dis.*, **38**, 725-732.
- Pryor, W.A. and Church, D.F. (1991): Aldehydes, hydrogen peroxide, and organic radicals as mediators of ozone toxicity. *Free Radic. Biol. Med.*, **11**, 41-46.
- Tsuda, S., Matsusaka, N., Ueno, S., Susa, N. and Sasaki, Y.F. (2000): The influence of antioxidants on cigarette smoke-induced DNA single-strand breaks in mouse organs: a preliminary study with the alkaline single cell gel electrophoresis assay. *Toxicol. Sci.*, **54**, 104-109.
- Tyagi, A.K., Nirala, B.K., Malik, A. and Singh, K. (2008): The effect of negative air ion exposure on *Escherichia coli* and *Pseudomonas fluorescens*. *J. Environ. Sci. Health A Tox. Hazard. Subst. Environ. Eng.*, **43**, 694-699.
- Vacchiano, C.A. and Tempel, G.E. (1994): Role of nonenzymatically generated prostanoid, 8-iso-PGF<sub>2</sub> alpha, in pulmonary oxygen toxicity. *J. Appl. Physiol.*, **77**, 2912-2917.
- Victorin, K. (1992): Review of the genotoxicity of ozone. *Mutat. Res.*, **277**, 221-238.



Letter

## Neurotoxicity of perfluorooctane sulfonate (PFOS) in rats and mice after single oral exposure

Itaru Sato<sup>1</sup>, Kosuke Kawamoto<sup>1</sup>, Yasuo Nishikawa<sup>1</sup>, Shuji Tsuda<sup>1</sup>, Midori Yoshida<sup>2</sup>,  
Kaori Yaegashi<sup>3</sup>, Norimitsu Saito<sup>3</sup>, Wei Liu<sup>4</sup> and Yihe Jin<sup>4</sup>

<sup>1</sup>Department of Veterinary Medicine, Iwate University, 3-18-8 Ueda, Morioka, Iwate 020-8550, Japan

<sup>2</sup>Division of Pathology, National Institute of Health Sciences, 1-18-1 Kamiyoga, Setagaya, Tokyo 158-8501, Japan

<sup>3</sup>Research Institute for Environmental Sciences and Public Health of Iwate Prefecture, 1-36-1 Iiokashinden, Morioka, Iwate 020-0852, Japan

<sup>4</sup>Department of Environmental Science and Technology, Dalian University of Technology, Linggong Road 2, Dalian, Liaoning 116024, China

(Received April 10, 2009; Accepted June 29, 2009)

**ABSTRACT** — Perfluorooctane sulfonate (PFOS) and perfluorooctanoate (PFOA) are widely used in industrial fields and consumer products, and are ubiquitously found in the environment and animal tissues. In the present study, their neurotoxicity was examined using rats and mice by means of neurobehavioral observation, histopathological inspection and chemical assays. PFOS and PFOA alone did not cause any neurotoxic symptoms up to their sublethal doses (PFOS: 500 mg/kg, PFOA: 1,000 mg/kg). However, tonic convulsions were caused in the PFOS-treated rats ( $\geq 250$  mg/kg) and mice ( $\geq 125$  mg/kg) when ultrasonic stimulus was applied to the animals. The same ultrasonic stimulus never induced convulsions in the control animals and in the animals treated with PFOA. Concentration of PFOS in the brain was considerably lower than in other tissue, but it seemed to increase gradually with time after exposure. No morphological changes were detected by histopathological examination of the brain. There were also no changes in concentrations of norepinephrine, dopamine, serotonin, glycine, 4-aminobutylic acid and glutamic acid in the brain. The present study revealed neurotoxic effects of PFOS in animals. Convulsive effect of PFOS may not be attributed to the quantitative alterations of neurotransmitters or lesions of nerve cells in the brain, although the mechanism of its neurotoxicity has not been cleared.

**Key words:** PFOS, PFOA, Neurotoxicity, Convulsion

### INTRODUCTION

Perfluorooctane sulfonate (PFOS) and perfluorooctanoate (PFOA) have been manufactured for several decades, and used for surfactants, polymers, water-repellents, lubricants, coating agents and as components of fire retardants, pharmaceuticals, cosmetics and insecticides. PFOS and PFOA are found ubiquitously in the global environment including surface water (Saito *et al.*, 2004; Hansen *et al.*, 2002) and wild life (Giesy and Kannan, 2001; Kannan *et al.*, 2001a, 2001b and 2002), because they are chemically stable and persistent in the environment. These chemicals are also detected from human sera who have not been exposed occupationally to these chemicals (Harada *et al.*, 2004; Jin *et al.*, 2007).

Significant toxicities of PFOS and PFOA, such as

hepatotoxicity (Butenhoff *et al.*, 2002; Seacat *et al.*, 2002, 2003), developmental or reproductive toxicity (Lau *et al.*, 2003, 2004; Thibodeaux *et al.*, 2003), and genotoxicity (Yao and Zhong, 2005) have been reported in recent years. Carcinogenicity to human is also suggested by epidemiological studies for workers employed in PFCs manufacturer (Alexander *et al.*, 2003; Gilliland and Mandel, 1993).

Austin *et al.* (2003) have reported that PFOS (i.p., 10 mg/kg for 2 weeks) increases norepinephrine concentration in the rat brain (Austin *et al.*, 2003). On the other hand, Harada *et al.* (2005) found that PFOS (10 and 20  $\mu$ M) affects action potential and L-type  $Ca^{2+}$  current of cell membrane (Harada *et al.*, 2005). These findings suggest that these chemicals have some effect on the nervous system, but there are few studies on the neurotoxicity of

Correspondence: Yihe Jin (E-mail: yihejin@cmu@hotmail.com)

PFOS and PFOA in animals. The purpose of this study is to examine the neurotoxicity of PFOS and PFOA by means of neurobehavioral observation, histopathological inspection, and chemical assays.

## MATERIALS AND METHODS

### Animals and reagents

Animal experiments were conducted in Iwate University and Dalian University of Technology. Six- or seven-weeks old male ICR mice and Wistar rats were purchased from Clea Japan Inc. (Tokyo, Japan) or Experimental Animal Care Center of Dalian Medical University (Dalian, China), and used for the experiments after 1 or 2-weeks acclimation. They were fed commercial diet (MF, Oriental Yeast Industries, Tokyo, Japan; or MF, Qianmin Feed Factory, Shenyang, China) and tap water throughout the acclimation and the experimental periods. The animal room was kept at  $23 \pm 1^\circ\text{C}$  with 12-hr light/dark cycle. Animal experiments were approved by the animal research committee, and were conducted according to the guidelines for animal experiment in each university.

PFOS (potassium salt, purity  $\geq 98\%$ ) and PFOA (purity  $\geq 90\%$ ) were purchased from Fluka Chemical GmbH (Buchs, Switzerland). Bulk of the other reagents were obtained from Wako Pure Chemical Industries (Osaka, Japan). PFOS and PFOA were dissolved in 2% carboxymethyl cellulose at appropriate concentrations for administration to animals.

### Neurobehavioral observation

Both rats and mice were used in this experiment. Two or 3 animals were assigned to each experimental group. PFOS (125-500 mg/kg) or PFOA (250-1,000 mg/kg) were administered orally to the animals. The maximum dose of each chemical was a sublethal dose determined by a preliminary experiment. Control animals were given vehicle. The animals were carefully observed for pharmacotoxic signs especially for excitability, such as straub tail, tremors, twitches, convulsions, restlessness, alertness and motor activities for 14 days. Responses such as startle response, touch response, pain response, righting reflex, visual placing, abdominal tone and limb tone were examined daily according to the method of Irwin (Irwin, 1967). As one of the external stimuli, ultrasonic stimulus (44 kHz, 10 sec) was applied to the animals once a day during the experimental period. The ultrasonic machine (B42-JK, Branson Ultrasonic Corporation, Danbury, CT, USA) was set 1 m apart from the animal cage. Rectum temperature and body weights were also measured during the observation period.

### Histopathological inspection

Twelve rats were divided into 4 groups and treated with oral administration of PFOS (0, 125, 250, 500 mg/kg). Twenty-four hours after exposure, the animals were deeply anesthetized with ether to collect the blood from vena cava. Serum samples were isolated by a conventional method, and stored in a freezer until use. Immediately after blood collection, the animals were euthanized by bleeding to collect the brain, liver, and kidney. The halved brain, portions of the liver and kidney were stored in a freezer for PFOS determination, and remaining tissues were fixed with 10% formalin neutral buffered solution. The cerebrum and cerebellum were transversely dissected. These organs fixed were embedded in paraffin wax, cut into 4  $\mu\text{m}$  sections and stained with hematoxylin and eosin for histopathological inspection. Serial sections of the brain were stained with luxol fast blue, and incubated with neurofilament protein (DAKO Japan, Kyoto, Japan) and GFAP (DAKO Japan) antibodies to detect any damage to neuronal or glial cells. After incubation, the section is allowed by the labeled polymer prepared by combining amino acid polymers with peroxidase and secondary antibody (Histofine Simple Stain Rat MAX-PO, Nichirei, Tokyo, Japan) and visualized by DAB chromogen.

### PFOS concentration

The tissues stored in a freezer were thawed and homogenized with 4 volumes of ultrapure water using a coaxial high-speed homogenizer (model 395, Dremel). One milliliter of these homogenates and sera were mixed with 1 ml of 0.5 M tetrabutylammonium hydrogensulfate (pH 10) and 2 ml of 0.25 M sodium carbonate, then stirred well. Five milliliter of methyl tert-butyl ether (MTBE) was added to the mixture, shaken for 1 min, and centrifuged for 10 min at 3,000 rpm to collect the MTBE layer. The aqueous layer was treated with MTBE once more. The first and second MTBE layers were combined, dried with nitrogen gas, dissolved in 1 ml of 90% methanol using ultrasonic machine, and filtered with 0.2  $\mu\text{m}$  nylon filter (Autovial, Whatman Japan, Tokyo, Japan). The filtrates were analyzed by LC/MS (Agilent 1100 LC/MSD, Agilent Technologies, Santa Clara, CA, USA) to determine the concentrations of PFOS in tissues. Conditions of LC/MS are shown below.

Column	ZORBAX XDB C-18 (2.1 mm $\times$ 150 mm, Agilent)
Eluent	10 mM Ammonium acetate:Acetonitrile = 55:45
Flow rate	0.2 ml/min.
Injection vol.	10 $\mu\text{l}$

## Neurotoxicity of PFOS in rats and mice.

Ionization	ESI (-)
Neblizer	N <sub>2</sub> (241 kPa)
Drying gas	N <sub>2</sub> (12.5 l/min)
Fragmentor	180 V
SIM (m/z)	498.9

To observe the time course changes of PFOS concentration, additional rats were treated with PFOS (125, 250, or 500 mg/kg, p.o.), and measured for its concentration in the brain 0.25, 0.5, 1, 3, 5 and 10 days after exposure.

### Neurotransmitters

Rats were euthanized 0, 24 or 48 hr after exposure to PFOS (250 mg/kg, p.o.) to collect the brain. Brain samples were cut lengthwise into two: one for catecholamines and the other for amino acids determinations. They were divided into the cerebrum and the cerebellum including pons and medulla to apply each assay.

**Catecholamines:** Samples were homogenized with 3 volumes of 2% perchloric acid (including 0.1 mM EDTA) and the same volume of internal standard solution (isoproterenol, 1 µg/ml in 2% perchloric acid). The homogenates were settled in a refrigerator for 10 min, and 200 µl of the supernatants was filtered with a centrifugal filter unit (Ultrafree-MC, 0.45 µm, Millipore, Bedford, MA, USA). The filtrates were mixed with 70 µl of 1 M sodium acetate to adjust its pH to 3, then assayed for norepinephrine, dopamine and serotonin by HPLC (Nanospace SI-2, Shiseido, Tokyo, Japan). The conditions of HPLC were as follows.

Column	Inertsil ODS-3 (3 mm × 5 cm, GL Science, Tokyo, Japan), 35°C
Eluent	a:b:c:d = 810:19:1:170 a) Acetate/citrate buffer (0.1 M sodium acetate:0.1 M citric acid = 9:10) b) Sodium octanesulfonate, 10 mg/ml in the buffer c) Na <sub>2</sub> -EDTA, 5 mg/ml in the buffer d) Methanol
Flow rate	0.6 ml/min
Injection vol.	10 µl
Detector	ECD (750 mV)

**Amino acids:** Glycine, glutamic acid and 4-aminobutylic acid (GABA) were measured by an amino acid autoanalyzer (JCL-500, JEOL, Tokyo, Japan). Assay samples were prepared similarly to the above experiment; but the deproteination was conducted with 3% sulfosalicylic acid, and the assay samples were diluted with the first eluent of this analyzer.

Effect of PFOS on glutamic acid oxidase was examined *in vitro* using an assay kit for glutamic acid (Yamasa Corporation, Chiba, Japan). PFOS was mixed with the

coloring solution, which contained glutamic acid oxidase, at concentrations of 0, 15, 50, 100 or 250 µg/ml. Glutamic acid (0.1 mg/ml, 0.2 ml) was added to this coloring solution to initiate the enzyme reaction, and the absorbance at 600 nm was immediately measured for 2 min with 15-sec intervals. The enzyme activity was estimated by the rate of absorbance increment.

### Statistical analyses

Fisher's exact test and Dunnett's t test were adopted as statistical methods. A p-value less than 0.05 was considered to be statistically significant.

## RESULTS

### Neurobehavioral observation

Animals treated with 250 mg/kg or more PFOS or PFOA showed decrease in body weight or delay of weight gain. There were no remarkable differences in rectum temperature (data not shown). Neither PFOS nor PFOA alone showed any symptoms that may suggest neurotoxicities to rats and mice up to their sublethal doses. The ultrasonic stimulus did not cause any distinct behavioral effect except for startle responses in control animals and animals treated with PFOA. However, some of the PFOS-treated rats (250 and 500 mg/kg) and mice (125 mg/kg and more) showed burst of locomotion just after the application of ultrasonic stimulus, and resulted in tonic convulsions within a few seconds. This effect of PFOS was statistically significant (Fisher's exact test).

The convulsions lasted about 30 sec. Some animals died without recovery from convulsions, some other animals recovered from convulsions but died within a few days, and the other animals recovered and survived during the experimental period (Table 1).

### Histopathological inspection

Any histopathological changes were not detected in the neuronal or glial cells of the cerebrum and the cerebellum stained with not only H-E, but also Luxol fast blue, neurofilament protein and GFAP in all the treated rats. In addition, no abnormalities were observed in the other organs (photos were omitted).

### PFOS concentration

Fig. 1A shows PFOS concentrations in rats sacrificed 24 hr after exposure. The highest concentration of PFOS was found in the liver, and the lowest was in the brain. Concentration/dose ratio of PFOS was 1.2-3.9 for the liver, 0.4-1.3 for the kidney and serum, and 0.05-0.1 for the brain. The concentration of PFOS was not clearly propor-

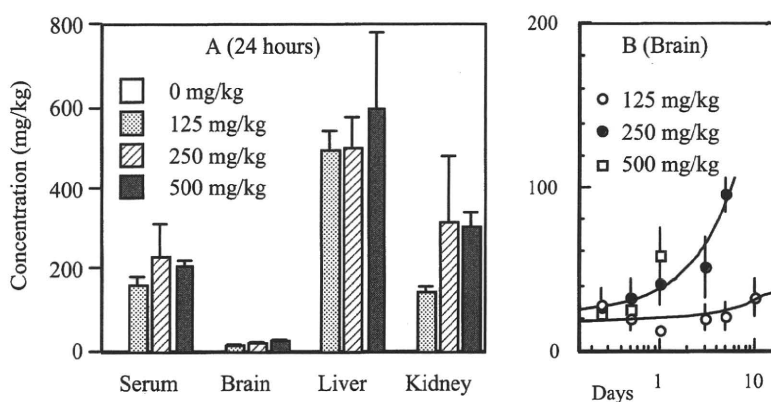
**Table 1.** Neurobehavioral effects of PFOS in rats and mice

Rats	Day	0.5	1	1.5	2	3	4	5	6	7	8	9	10	11	12	13	14
125 mg/kg	No.1	-	-	-	-	-	-	-	-	-	-	-	-	-	-	-	-
	No.2	-	-	-	-	-	-	-	-	-	-	-	-	-	-	-	-
250 mg/kg	No.1	-	-	-	-	-	△	△	-	×							
	No.2	-	-	-	-	-	△	△	△	△	-	-	-	-	-	-	-
	No.3	-	-	-	+	+	+	-	-	-	-	-	-	-	-	-	-
500 mg/kg	No.1	-	-	△	△	×											
	No.2	-	-	-	+	△	×										

Mice	Day	0.5	1	1.5	2	3	4	5	6	7	8	9	10	11	12	13	14
125 mg/kg	No.1	-	-	-	-	-	-	-	-	-	-	-	-	-	-	-	-
	No.2	-	△-×														
	No.3	-	-	-	-	-	-	-	-	-	-	-	-	-	-	-	-
250 mg/kg	No.1	-	-	△	-	-	-	-	-	-	-	-	-	-	-	-	-
	No.2	-	-	-	-	-	-	-	-	-	-	-	-	-	-	-	-
	No.3	-	-	△-×													
500 mg/kg	No.1	-	-	-	-	-	-	-	-	-	-	-	-	-	-	-	-
	No.2	-	-	△-×													

-: no visible change. +: excited locomotion. △: convulsion, ×: death. Data for the control animals were omitted, as there were no visible changes.



**Fig. 1.** PFOS concentrations in rats. A: 24 hr after exposure to PFOS (mean  $\pm$  S.D. for 3 rats). B: Time course changes in the brain (mean  $\pm$  S.D. for 5 rats). Curves are regression lines for the 125 mg/kg and 250 mg/kg groups.

tional to its dose in every tissue.

Fig. 1B shows time-course changes of PFOS concentration in the rat brain. The concentration at 3 hr after administration was 20-25 mg/kg regardless of its dose. However, it showed increasing tendency except for the 125 mg/kg group, and the 250 mg/kg group reached about

100 mg/kg 5 days after administration. Obvious declines were not observed during the experimental period. In this experiment, many of the animals treated with 250 or 500 mg/kg had died by 10 days or 3 days after exposure, respectively.